A&A 391, 1159–1165 (2002)
DOI: 10.1051/0004-6361:20020882

Astronomy & Astrophysics

Dissociative recombination of $C_2H_3^+$

S. Kalhori[1], A. A. Viggiano[2], S. T. Arnold[2], S. Rosén[1], J. Semaniak[3], A. M. Derkatch[1], M. af Ugglas[4], and M. Larsson[1]

[1] Department of Physics, Stockholm University, SCFAB, 106 91 Stockholm, Sweden
[2] Air Force Research Laboratory, Space Vehicles Directorate, 29 Randolph Rd, Hanscom AFB, MA 01731, USA
e-mail: Albert.Viggiano@hanscom.af.mil
[3] Institute of Physics, Świętokrzyska Academy, 25-406 Kielce, Poland
e-mail: jacek@pu.kielce.pl
[4] Manne Siegbahn Laboratory, Stockholm University, 104 05 Stockholm, Sweden
e-mail: ugglas@msi.se

Received 23 April 2002 / Accepted 10 June 2002

Abstract. We have studied the vibrationally relaxed $C_2H_3^+$ ion in the heavy – ion storage ring CRYRING in Stockholm. We measured the dissociative recombination absolute cross section over center-of-mass energies in the range between 0 and 0.1 eV by scanning the electron energy.
The rate of different neutral product channels of dissociative recombination was measured. We found the three-body channel C_2H + H + H, with a branching ratio of 59%, to be the dominant one. Finally, we compare $C_2H_3^+$ and $C_2H_2^+$ (Derkatch et al. 1999) results.

Key words. molecular processes – ISM: molecules – ISM: clouds

1. Introduction

Molecular synthesis within interstellar clouds is governed primarily by ion chemistry (Adams & Smith 1988; Millar et al. 1997; Smith & Spanel 1995). The significant role attributed to ions results from a combination of the low temperatures involved (10–100 K) and the barrierless nature of chemical reactions involving ions. While neutral reactions often proceed slowly at low temperature due to activation barriers, ion reactions generally exhibit either no dependence or a negative dependence on temperature (Ikezoe et al. 1986). Within interstellar clouds, ions are initially formed by cosmic-ray ionization of the predominant neutral species, which is generally molecular hydrogen (Adams & Smith 1988; Millar et al. 1997; Smith & Spanel 1995). The resulting H_2^+ ion reacts readily with an additional H_2 molecule to form H_3^+, a species that initiates subsequent synthetic pathways. The primary loss mechanisms for molecular ions in interstellar clouds are ion-neutral reactions and dissociative recombination (DR), a rapid process wherein the ion captures an incident electron, thus forming an excited state along which the molecule can dissociate into two or more neutral fragments.

It has been possible to measure the rate constants or cross sections of DR reactions for many years; for all except the simplest systems, the reactions were found to be extremely rapid. These measurements demonstrated potential synthetic routes for numerous molecules that were known to exist within the interstellar clouds (Winnewisser & Herbst 1993). Only recently has it become possible to measure the neutral product distribution resulting from DR, primarily due to the advent of storage rings (Larsson & Thomas 2001). Early storage ring studies on small ions showed that dissociations which resulted in the formation of three neutral products were more prevalent than previously thought, indicating the need for further experimental measurements.

This paper reports on the dissociative recombination of $C_2H_3^+$. This ion is formed in interstellar clouds by, for example, proton transfer reactions with the acetylene molecule (Millar et al. 1997):

$$H_3^+ + CO \rightarrow HCO^+ + H_2 \quad (1)$$

$$HCO^+ + C_2H_2 \rightarrow C_2H_3^+ + CO. \quad (2)$$

Dissociative recombination rate constants are reported as a function of translational energy, and a product distribution at near zero translational energy is also reported. This is one of the largest ions studied to date for which the products of DR have been determined (Larsson & Thomas 2001).

In addition to having implications for the modeling of interstellar clouds, the overall degree of fragmentation that occurs upon recombination of organic ions is also of interest to researchers exploring the application of plasmas to combustion systems. Modeling results have shown that

Send offprint requests to: S. Kalhori, e-mail: shiri@physto.se

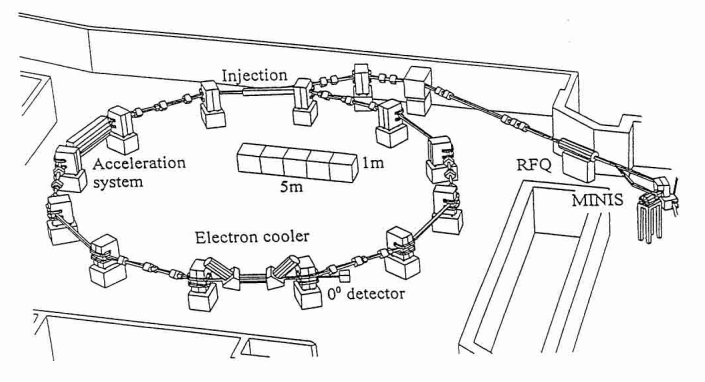

Fig. 1. A view of the CRYRING facility at Manne Siegbahn Laboratory.

maintaining high levels of ionization within a hypersonic combustor system may effectively improve combustor performance (Williams et al. 2000; Williams et al. 2001). The production of hydrocarbon radicals via DR was found to be a key factor in the observed enhancement. To date, the models have assumed formation of two products in all DR reactions. However, if the production of three neutrals upon DR were shown to be a significant channel, the models would predict an even greater enhancement due to the plasma.

2. Experiment

The experiment was performed at the heavy ion storage ring CRYRING at the Manne Siegbahn Laboratory in Stockholm. The experimental setup and data analysis procedure have been described previously in detail (Strömholm et al. 1996; Neau et al. 2000). Here we only give a brief description and concentrate on issues attributed to the specifics of the present experiment.

Figure 1 shows the layout of the storage ring. The $C_2H_3^+$ ions are produced in a hot-filament discharge ion source (MINIS). In this ion source it is expected that two isomers of $C_2H_3^+$ can be produced, one is a classical linear structure, and the other is a non-classical bridged form. Figure 2 illustrates these two isomers (Weber et al. 1976), which are separated in energy by 5 kJ mol^{-1} (0.05 eV). Experiments only start after 4–5 s so that an equilibrium mixture is likely. After extraction from the source, the ions are accelerated to 40 keV, passed through a dipole magnet, which serves as a mass separator and then injected into the storage ring. The ring, which has a circumference of $c = 51.6$ m, consists of twelve straight sections separated by bending magnets. One of the sections is equipped with a radiofrequency acceleration system. The ions are accelerated to the maximum energy of $E = 3.56$ MeV, which is limited by the magnetic rigidity of the storage ring. After acceleration, the ions periodically penetrate a uniform, average-velocity merged electron beam, which is confined to a diameter of 4 cm by a solenoidal magnetic field over an effective interaction length, l, equal to 85 cm. The electron beam is steered in and out of the interaction region by a couple of toroidal fields. In the present experiment an electron beam with a density of 1.3×10^6 cm^{-3} is used.

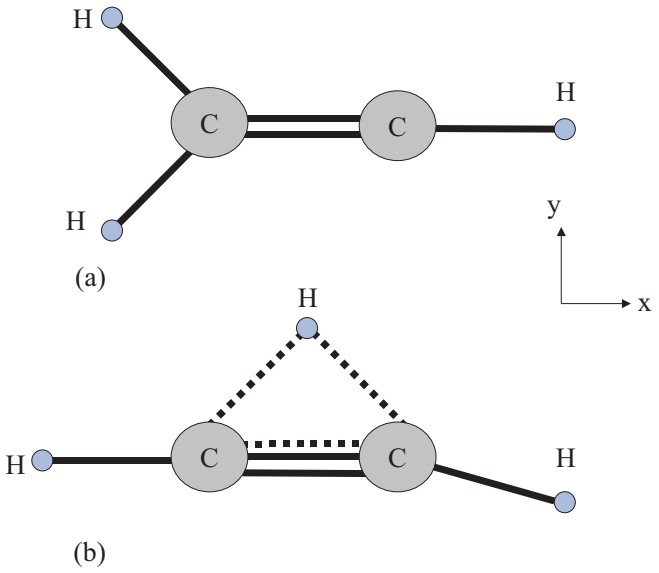

Fig. 2. Molecular structures for vinyl cation $C_2H_3^+$: **a)** classical; **b)** bridged.

The velocity distribution of the electrons in the rest frame of the moving ions is described by a flattened Maxwell distribution characterized by different electron temperatures in the directions parallel, $kT_\parallel$, and transverse, $kT_\perp$, to the ion beam (Danared et al. 1994). The transverse electron beam temperature, being originally as high as $kT_\perp = 100$ meV (which is determined by the cathode temperature, 1200 K), is reduced to about 2 meV, prior to entering the interaction region by using adiabatic expansion of the electron beam in a decreasing magnetic field (Danared et al. 1998). The longitudinal energy spread of the accelerated electrons is about 0.1 meV. In the interaction region, the heat from the ion beam is transferred to the cold, average-velocity matched, continuously renewed electron beam via Coulomb interactions between the electrons and the ions. It leads to reduction of the momentum spread of the ion beam. As a result, the ion beam, confined by the magnetic fields in the ring, shrinks in diameter. Under such circumstances a typical storage time of the ion-beam is about 10 s and after this time the beam is dumped and a new injection cycle starts. An important advantage of such a long storage time is that the ions have sufficient time to relax vibrationally via infrared emission.

Apart from cooling the ions, the electron beam serves as a high density target for electron – ion recombination experiments. These reactions can be studied as a function of collision energy in the center-of-mass frame, which can be easily varied by altering the velocity of the electrons in the laboratory frame. The effective collision energy is dependent on the difference between the average velocities of the electrons and the ions (called the detuning velocity, v_d). Nonrelativistically it is given by $E_{cm} = m_e v_d/2$, where m_e is the electron mass. The collision energy fulfils the following relation

$$E_{cm} = \left(\sqrt{E_e} - \sqrt{E_{cool}}\right)^2, \quad (3)$$

where E_{cool} is the electron energy for the cooling condition, which is determined experimentally by reading the Schottky

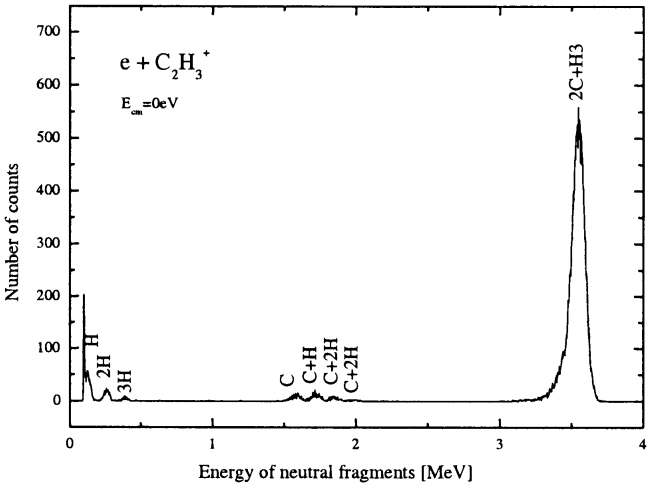

Fig. 3. Energy spectrum of neutral fragments from DR of $C_2H_3^+$ measured at 0 eV collision energy.

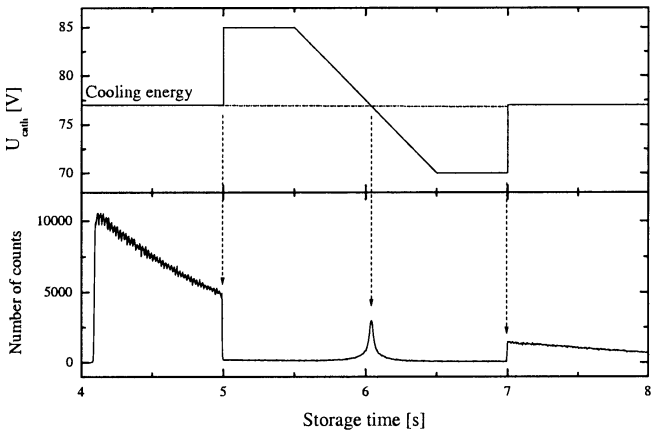

Fig. 4. The electron energy in the laboratory frame of reference is varied by ramping the electron gun cathode voltage (top). The corresponding spectrum (bottom) represents the events which result in detection of at least two carbon atoms.

signal frequency. The electron energy, E_e, is defined by the cathode voltage corrected for its contact potential, the electron space charge potential (Andersen et al. 1990), and its partial neutralization due to ions that are created in collisions between residual gas molecules and electrons in the interaction region then trapped in electron space charge potential (Semaniak et al. 1998). Neutral atoms or molecules, which are produced in the interaction region, are separated from the parent ion beam in the first bending magnet after the electron cooler section. The neutral particles follow a straight line and arrive in an ion-implanted charge-particle detector, which detects the fragments with 100% efficiency. The detector measures the energy of the arriving fragments yielding an analog signal whose amplitude is proportional to the deposited energy. The signal is amplified and converted into the corresponding channel number with an AD converter, which constitutes an integral part of a multichannel analyzer (MCA). The MCA is used to record the pulse height spectrum. Since all fragments which originate from the same dissociation event arrive in the detector within a time interval of a few nanoseconds, i.e. much shorter than the charge collection time in the detector (typically of the order of microseconds), they are detected at the full energy of the ion beam. Figure 3 shows a pulse height spectrum measured at the velocity-matching condition.

Alternatively, the count rate in a given pulse height range can be measured as a function of storage time with a multichannel scaler (MCS) coupled with a single channel analyzer (SCA). It allows one to follow DR count rate vs. collision energy which can be continuously altered as a function of storage time.

3. Data analysis

3.1. Dissociative recombination cross section

The measurement is performed after 5 s of cooling time, which is long enough to allow the ions to relax through infrared emission to their vibrational ground state. The DR cross sections are studied over center-of-mass energies ranging between 0 eV and 0.1 eV by scanning the electron energy. First, the cathode voltage is rapidly increased to a specified maximum value and then linearly decreased to the minimum value while crossing the cooling voltage in between. It is possible to study DR reactions at the same center-of-mass energies where the electron beam moves both faster and slower than the ions. The rate at which neutral products of DR reactions are detected, $C_{DR}(t)$, is proportional to the corresponding rate coefficient, $\langle \sigma v \rangle$, which is essentially the cross section averaged over a flattened Maxwellian electron velocity distribution (Danared et al. 1994):

$$\langle \sigma v \rangle = \frac{c}{n_e l} \frac{C_{DR}(t)}{N_i(t)}, \tag{4}$$

where $N_i(t)$ is the number of ions as a function of storage time. The count rate $C_{DR}(t)$ was measured with a single channel analyzer connected to a multichannel scaler. However, it was not possible to resolve the pure DR signal from a background, generated by neutral products of other reactions (collisions of the ions with residual gas molecules), which include at least two carbon atoms. Thus, the high and low discrimination levels in the SCA are chosen to register all pulses with amplitudes characteristic for detection of at least two carbon atoms. Figure 4 shows both the electron energy scan and the MCS spectrum, which was measured during 2200 injection cycles. A part of the scan, corresponding to high center-of-mass energies at which DR cross sections are negligibly small, gives a direct measure of the collisional background. After its interpolation over the entire scan, the pure DR count rate, $C_{DR}(t)$, is easily derived.

The number of ions circulating in the ring cannot be measured at the same time as the DR signal since this requires a much more intense beam than the silicon detector (exposed from intense flux of DR products) can handle. Therefore, the part of the spectrum which is fully dominated by the background, is also used as an indirect measure of the ion beam intensity. Then, in an independent experiment a count rate of the collisional background, which is measured after turning the electron beam off, is related to the ion current.

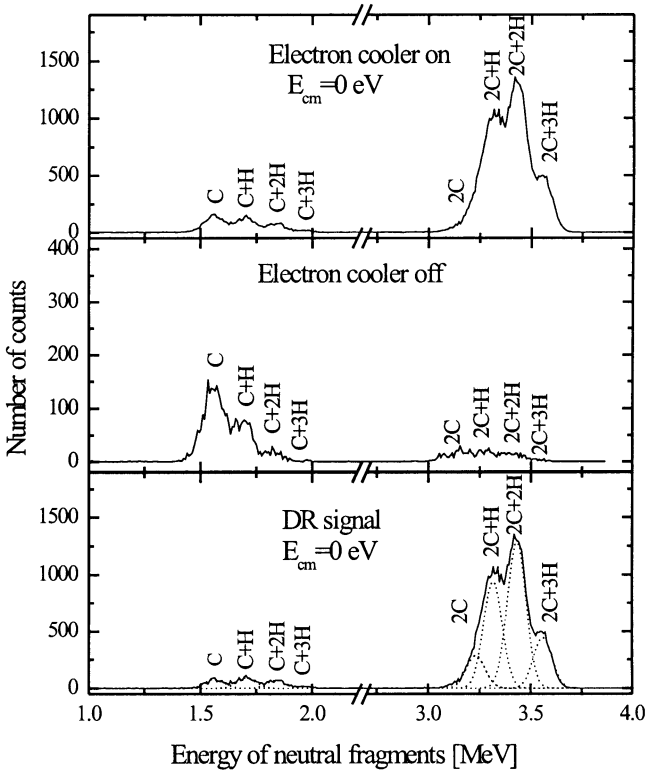

Fig. 5. Energy spectra of neutral fragments from DR of $C_2H_3^+$ measured with a grid in front of the detector. *Top*: Spectrum measured at 0 eV collision energy. *Middle*: Background spectrum measured after turning the electron beam off. *Bottom*: DR spectrum obtained after subtracting the background contribution.

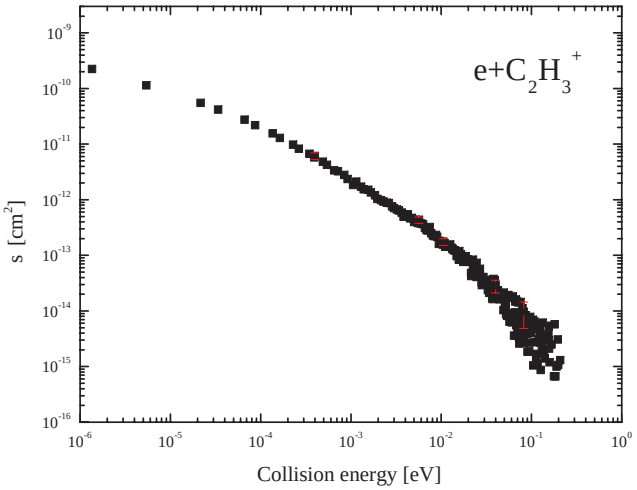

Fig. 6. Absolute DR cross section for $C_2H_3^+$ as a function of collision energy obtained by dividing the measured rate coefficient by the detuning velocity.

The absolute cross sections are obtained after dividing the measured rate coefficient by the detuning velocity, as shown in Fig. 6. Independently, they are derived by unfolding the measured rate coefficient with a numerical Fourier transform (Strömholm et al. 1996). The DR cross sections are corrected for the DR events that occur in the toroidal section of the electron cooler, where non-zero angles between the ion and the electron beams make collision energies different than in the straight section of the electron cooler (Lampert et al. 1996).

3.2. Dissociative recombination branching fractions

In order to study products in DR of $C_2H_3^+$ the experimental setup is modified by inserting a grid with known transmission ($T = 0.297 \pm 0.015$) in front of the silicon detector mentioned above. The grid is made of steel, 50 μm thick, and has holes of 70 μm in diameter. Each fragment that arrives in it can be stopped with a probability of $(1 - T)$ or pass through it with a probability of T. Thus, the products of any DR reaction that contain at least two neutral fragments (as can be seen from Eq. (6)) will be detected with a different probability and consequently with different energy carried by the fragments that pass through the grid. For example the products C_2H_2+H can be either detected with a probability of T^2 at the full ion beam energy, or with a probability of $T(1 - T)$ at the energy carried by one of the fragments. Thus the DR neutral fragments spectrum, which is measured with the MCA, becomes distributed over a series of peaks as shown in Fig. 5.

Their intensities are directly related to detection probabilities (expressed in terms of transmission T) and branching ratios. The spectra are measured at 0 eV center-of-mass energy, within short time intervals preceded by 0.5 s time periods during which the electron beam is turned off in order to minimize the possible increase of the background that results from collisions of the ions in the beam with the ions trapped in the electron space charge potential. Independently, the neutral product spectra are recorded after turning the electron beam off. Thus, the collisional background spectrum can be obtained and subtracted from the previously measured spectrum after normalizing to the ion beam intensity, as is done in the cross section measurement. After subtraction of the background, we obtain the following linear matrix equation relating the number of events in different dissociation channels N_α, N_β, N_γ, N_δ, N_ϵ, N_ε to the number of counts in individual peaks N_{2C+3H}, N_{2C+2H}, N_{2C+H}, N_{2C}, N_{C+3H}, N_{C+2H}, N_{C+H}, N_C, N_{2H}:

The peaks are not completely separated; therefore, the number of counts in the individual peaks is obtained by fitting a Gaussian curve to each peak. The branching fraction for each dissociation channel is obtained after normalization, e.g. $\alpha = N_\alpha/(N_\alpha + N_\beta + N_\gamma + N_\delta + N_\epsilon + N_\varepsilon)$.

4. Results and discussion

4.1. Dissociative recombination cross section

The total cross section for DR of $C_2H_3^+$ is shown in Fig. 6 over a collisional energy range from 10^{-6} to 10^{-1} eV. The total error in the cross section is about 20% at low energies; this limit is based on uncertainties in the ion beam current (15%), the effective length of the electron cooler (7%), and the electron density (7%). Above approximately 1 meV, the data become scattered due to weak signals and a relatively large background signal subtraction. The errors are mainly represented by the scatter in the data, i.e. statistical variations. Errors in the energy are

$$\begin{pmatrix} N_{2C+3H} \\ N_{2C+2H} \\ N_{2C+H} \\ N_{2C} \\ N_{C+3H} \\ N_{C+2H} \\ N_{C+H} \\ N_{C} \\ N_{2H} \end{pmatrix} = \begin{pmatrix} T^2 & T^2 & T^3 & T^3 & T^2 & T^2 \\ T(1-T) & 0 & 2T^2(1-T) & T^2(1-T) & 0 & 0 \\ 0 & T(1-T) & T(1-T)^2 & T^2(1-T) & 0 & 0 \\ 0 & 0 & 0 & T(1-T)^2 & 0 & 0 \\ 0 & 0 & 0 & 0 & T(1-T) & 0 \\ 0 & 0 & 0 & 0 & 0 & T(1-T) \\ 0 & 0 & 0 & 0 & 0 & T(1-T) \\ 0 & 0 & 0 & 0 & T(1-T) & 0 \\ 0 & T(1-T) & T^2(1-T) & T(1-T)^2 & 0 & 0 \end{pmatrix} \begin{pmatrix} N_\alpha \\ N_\beta \\ N_\gamma \\ N_\delta \\ N_\epsilon \\ N_\varepsilon \end{pmatrix} \quad (5)$$

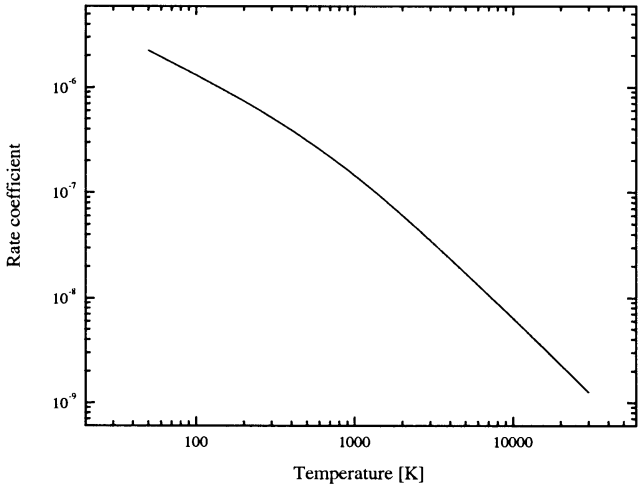

Fig. 7. Thermal rate coefficient for DR of $C_2H_3^+$ as a function of electron temperature.

estimated to be 0.5 meV at the lowest collision energies and up to 3 meV at the highest energies. They are mostly attributed to the finite width of the time (energy) windows in the MCS spectra. The cross section decreases rapidly with increasing collision energy and can be represented by a power law with an energy dependence of $E^{-1.36}$. This is larger than the $E^{-1.0}$ dependence applicable to the direct mechanism for DR. The total cross sections are larger than those recently found for $HCNH^+$, and the energy dependence is also larger. Integrating the measured cross sections yields rate constants as a function of translational temperature, the most useful way to represent the data for modeling purposes. The results are shown in Fig. 7. The data are curved on this plot with a break just below 1000 K. The higher translational temperature data follow a $T^{-1.38}$ dependence, and the low temperature data follow a $T^{-0.84}$ dependence being as high as 5×10^{-7} cm^3 s^{-1} at 300 K. The break may indicate a change in mechanism.

4.2. Dissociative recombination branching fractions

For dissociative recombination of $C_2H_3^+$, six product channels are energetically accessible (Mallard & Linstrom 2001):

$$C_2H_3^+ + e \rightarrow \begin{array}{ll} C_2H_2 + H + 6.74\ \text{eV}, & (\alpha), \\ C_2H + H_2 + 5.59\ \text{eV}, & (\beta), \\ C_2H + H + H + 1.07\ \text{eV}, & (\gamma), \\ C_2 + H + H_2 + 0.40\ \text{eV}, & (\delta), \\ CH_3 + C + 2.39\ \text{eV}, & (\epsilon), \\ CH_2 + CH + 1.17\ \text{eV}, & (\varepsilon). \end{array} \quad (6)$$

Channels α, β, γ and δ involve only C–H bond dissociations, corresponding to the loss of 1–3 hydrogen atoms, while channels ϵ and ε involve C–C bond dissociations. All six channels were found to have a non-zero contribution at a translational energy of near zero; the branching ratios are shown in Table 1.

The C–H bond dissociation channels (α–δ) account for 97% of the total reactivity. Although loss of a single H atom is the most exothermic reaction pathway, the branching ratio for that channel is only 29%. The dominant product channel is γ, the three-body product channel yielding two H atoms, with a branching ratio of 59%. The related two-body product channel (β), in which an H_2 molecule is subsequently formed, accounts for another 6% of the reaction products. The channels in which two H atoms are lost from $C_2H_3^+$ represent nearly two thirds of the total reactivity. Dissociation corresponding to the loss of all three H atoms from the carbon skeleton is exothermic only if an H_2 molecule is subsequently formed, as shown in reaction δ. This three-body product channel is observed with a minor branching ratio of 3%.

The branching ratios for both C–C bond dissociation channels are small. Channel ε, which involves a direct C–C cleavage, represents only 3% of the total reactivity. Channel ϵ which represents only 0.6% of the overall reactivity, must involve either molecular isomerization from CH_2=CH to CH_3–C prior to C–C cleavage or H transfer from CH to CH_2 after cleavage. Although channel ϵ is more exothermic than the direct C–C cleavage channel (ε), the branching fraction is smaller, perhaps due to the existence of a barrier associated with the hydrogen rearrangement (Weber et al. 1976).

Overall, a surprisingly large 62% of the reactivity results in the formation of three-body products. Possible mechanisms for explaining the formation of three-body product channels from DR of polyatomic ions have been discussed previously (Herbst & Lee 1997). While the primary products of reaction are thought to result from two-body channels, secondary fragmentation may occur if the primary products either retain sufficient vibrational energy or are formed in an excited electronic state. Given the large exothermicity of the primary two-body product channel (α), it seems likely that channel γ results from unimolecular decay of vibrationally or electronically excited $C_2H_2^*$.

The degree of fragmentation observed from DR of $C_2H_3^+$ is significantly larger than what has previously been assumed for this molecular ion. The gas-phase chemistry model for interstellar clouds by Herbst and Lee (HL_{old} in Table 1) (Herbst & Lee 1997) initially assigned a product distribution

Table 1. Product distributions for the dissociative recombination of $C_2H_3^+$ (this work) and $C_2H_2^+$ (Derkatch et al. 1999). Similar product channels are listed on the same row. Where HL_{old} and HL_{new} are taken from (Herbst & Lee 1997).

		$C_2H_3^+$					$C_2H_2^+$	
Mechanism	Products	$-\Delta H$	*Expt*	HL_{old}	HL_{new}	Products	$-\Delta H$	*Expt*
H loss	(α) C_2H_2+H	6.74	0.29(0.04)	0.50	0.30	C_2H+H	5.8	0.50 (0.06)
H_2 loss	(β) C_2H+H_2	5.59	0.06(0.03)	0.50	0.23	C_2+H_2	5.1	0.02 (0.03)
2H loss	(γ) C_2H+H+H	1.07	0.59(0.06)		0.23	C_2+2H	0.2	0.30 (0.05)
H+H_2 loss	(δ) C_2+H+H_2	0.40	0.03(0.01)					
C–C cleavage + isomerization	(ϵ) CH_3+C	2.39	0.006(0.002)			CH_2+C	2.4	0.05 (0.01)
C–C cleavage	(ε) CH_2+CH	1.17	0.03(0.01)		0.23	CH+CH	1.2	0.13 (0.01)

that was equally divided between only two channels: H and H_2 loss (Table 1 in Herbst & Lee 1997). While this model correctly identified C–H dissociation as the predominant DR mechanism for $C_2H_3^+$, it did not include any contribution from three-body product channels, i.e., 2H loss. The model was later updated (HL_{new} in Table 1) by Herbst & Lee (1997) to reflect the first branching ratio studies conducted in storage rings, which showed larger than expected amounts of three-body product channels. For $C_2H_3^+$, the two-body product channel corresponding to the loss of one hydrogen was assigned a branching ratio of 30% based on the storage ring DR results for H_3O^+. This assignment agrees well with the present $C_2H_3^+$ experimental measurement. The remaining assignments in HL_{new}, however, do not agree with the experimental measurement. The channel in which 2 H atoms are formed, and the related channel where H_2 is formed, were both assigned branching ratios of 23%, which significantly underestimates the contribution of three-body product channels. The updated model also assumed that C–C bond dissociations would be more significant than had been considered previously. The direct C–C bond dissociation channel was assigned a branching ratio of 0.23. This considerably overestimates the degree to which the carbon skeleton is broken during DR. Compared to the model inputs, the experimental results suggest that DR of $C_2H_3^+$ produces (a) more H atoms, together with less saturated carbon species, and (b) fewer one-carbon species.

In order to investigate how general the $C_2H_3^+$ results may be with regard to DR of other small organic ions, the present results are compared to the recently published results for $C_2H_2^+$ (Derkatch et al. 1999). To facilitate a comparison of the two DR processes, products that result from similar bond cleavages are shown on the same row in Table 1. The $C_2H_2^+$ DR channels that correspond to a loss of one or two H atoms are the most significant product channels, as was also observed for $C_2H_3^+$. However, the relative significance of those channels is reversed for the two molecular ions being considered. Specifically, the two-body dissociation resulting in a loss of only one H atom accounts for 50% of the $C_2H_2^+$ reactivity, compared to only 30% for $C_2H_3^+$, while production of two H atoms accounts for 59% of the $C_2H_3^+$ reactivity, compared to only 30% for $C_2H_2^+$. The smaller two H atom loss associated with the DR of $C_2H_2^+$ is likely a result of energetic considerations. The exothermicities associated with the loss of two H atoms from $C_2H_3^+$ and $C_2H_2^+$ are 1.07 and 0.2 eV, respectively. The smaller exothermicity for $C_2H_2^+$ leads to fewer exothermic phase space channels, which is manifested as a smaller branching ratio. Given the small exothermicity, it is actually somewhat surprising that two H atoms are lost in approximately one third of the $C_2H_2^+$ DR reactions. Loss of two H atoms followed by formation of H_2 is a minor channel for both systems, with branching ratios approximately 7–10% of that associated with the loss of 2 H atoms.

A large difference is noted between $C_2H_2^+$ and $C_2H_3^+$ DR with regard to the C–C bond dissociation channels. Both the direct bond cleavage and the bond cleavage coupled with hydrogen rearrangement channels are at least four times more prevalent for $C_2H_2^+$ than for $C_2H_3^+$ although the exothermicities are the same. The only simple explanation is that the more exothermic C–H bond dissociation channels in $C_2H_3^+$ compete more effectively with the C–C bond dissociation channels, thereby reducing the branching ratios for the latter channels. The competition between C–C and C–H bond dissociations will be explored further with more saturated compounds such as $C_2H_5^+$, where the C–C dissociation channels are also more exothermic.

The $C_2H_3^+$ ion shows a preference for three-body product dissociation, 62% overall, which is approximately twice as much as noted in DR of $C_2H_2^+$. As the comparison between these related species demonstrates, it is difficult at this time to generalize the present results to a wide variety of hydrocarbon ions. Future experiments with hydrocarbon ions will explore the competition between C–H and C–C bond dissociations and also the possibility of exothermic four-body product channels.

In addition to having clear astrophysical significance, the storage ring results for DR of small organic ions are also vital inputs for models exploring the enhancing effects of plasmas on combustion (Williams et al. 2000; Williams et al. 2001). Previously, such models have assumed a maximum number of two products resulting from DR of such ions, and generally, one of the neutrals was assumed to be a stable neutral molecule, i.e., not a radical species. However, the experimental results for $C_2H_2^+$ and $C_2H_3^+$ indicate the average number of neutral radicals produced upon DR is 2.24 and 2.28, respectively. It is interesting that the two systems have large differences in the individual channels, yet the average number of radicals produced is essentially the same. Because the reported enhancing effect from plasmas is strongly correlated to the concentration of radical species, this larger than expected number of radicals being

produced upon DR suggests that revised models will predict an even greater enhancing effect.

Acknowledgements. The authors would like to acknowledge the staff members of the Manne Siegbahn Laboratory for valuable help during the experiment. This work has been supported by the EORD under contract F61775-01-WE035 and IHP Programme of the EC under contract HPRN-CT-2000-00142. J.S. was supported in part by the State Committee for Scientific Research (Poland), under contract 146/E-346/SPUB-M/5. AAV and STA acknowledge financial support provided by the United States Air Force Office of Scientific Research under Project No. 2303EP4.

References

Adams, N. G., & Smith 1988, in Rate Coefficients in Astrochemistry, ed. T. J. Millar., & D. A. Williams (The Netherlands: Kluwer Academic Publishers), 173

Andersen, L. H., Bolko, J., & Kvistgaard, P. 1990, Phys. Rev. A, 41, 1293

Danared, H., Andler, G., Bagge, L., et al. 1994, Phys. Rev. Lett., 72, 3775

Danared, H., Källberg, A., Liljeby, L., et al. 1998, in Proc. Sixth European Particle Accelerator Conf., ed. S. Myers, L. Liljeby, Ch. Petit-Jean-Genaz, J. Poole, & K.-G. Rensfelt (London: IOP), 1031

Derkatch, A. M., Al-Khalili, A., Vikor, L., et al. 1999, J. Phys. B., 32, 3391

Herbst, E., & Lee, H. H. 1997, ApJ, 485, 689

Ikezoe, Y., Matsuoka, S., Takebe, M., & Viggiano, A. A. 1987, Gas Phase Ion-Molecule Reaction Rate Constants Through 1986, (Tokyo: Maruzen Company, Ltd.)

Lampert, A., Wolf, A., Habs, D., et al. 1996, Phys. Rev. A, 53, 1413

Larsson, M., & Thomas, R. 2001, Phys. Chem. Chem. Phys., 3, 4471

Mallard, W. G., & Linstrom, P. J., (eds.) 2001, NIST Chemistry WebBook, NIST Standard Ref. Database No. 69, National Institutes of Standards and Technology, (Gaithersburg, MD)

Millar, T. J., Farguahr, P. R. A., & Willacy, K. 1997, A&AS, 121, 139

Neau, A., Al Khalili, A., Rosén, S., et al. 2000, J. Chem. Phys., 113, 1762

Semaniak, J., Larson, Å., Le Padellec, A., et al. 1998, ApJ, 498, 886

Smith, D. & Spanel, P. 1995, Mass Spectrom. Rev., 14, 255

Strömholm, C., Semaniak, J., Rosén, S., et al. 1996, Phys. Rev. A, 54, 3086

Weber, J., Yoshimine M., & McLean D. 1976, J. Chem. Phys., 64(10), 4159

Williams, S., Bench, P. M., Midey, A. J., et al. 2000, in JANNAF 25th Airbreathing Propulsion Meet., Detailed Ion Kinetic Mechanisms for Hydrocarbon Air Combustion Chemistry (Monterey, CA)

Williams, S., Midey, A. J., Arnold, S. T., et al. 2001, in AIAA 4th Weakly Ionized Gases Workshop, Progress on the investigation of the effects of ionization on hydrocarbon/air combustion chemistry: kinetics and thermodynamics of C6-C10 hydrocarbon ions (Anaheim, CA)

Winnewisser, G., & Herbst, E. 1993, Rep. Prog. Phys., 56, 1209